Syntheses and Characterization of Polystyrene-Supported 2,5-Dimercapto-1,3,4-thiodiazole and Its Sorption Behavior for Pd(II), Pt(IV), and Au(III)

Rongjun Qu,[1,2] Changmei Sun,[1,2] Chunnuan Ji,[1] Chunhua Wang,[1] Qiang Xu,[1] Shulai Lu,[2] Changfeng Li,[1] Gang Xu,[1] Guoxiang Cheng[2]

[1]*School of Chemistry and Materials Science, Yantai Normal University, Yantai 264025, People's Republic of China*
[2]*School of Materials Science & Engineering, Tianjin University, Tianjin 300072, People's Republic of China*

Received 5 January 2005; accepted 11 July 2005
DOI 10.1002/app.23598
Published online in Wiley InterScience (www.interscience.wiley.com).

ABSTRACT: A type of chelating resin crosslinking polystyrene-supported 2,5-dimercapto-1,3,4-thiodiazole (also called bismuththiol I, BMT), containing sulfur and nitrogen atoms, was prepared. The structure of PS-BMT was confirmed by FTIR, elemental analysis, and X-ray photoelectron spectroscopy (XPS). Adsorption of Pd(II), Pt(IV), and Au(III) was investigated. The capacity of PS-BMT to adsorb Pd(II) and Pt(IV) was 0.190 and 0.033 mmol/g, respectively. The adsorption dynamics of Pd(II) showed that adsorption was controlled by liquid film diffusion and that the apparent activation energy, E_a, was 32.67 kJ/mol. The Langmuir model was better than the Freundlich model in describing the isothermal process of Pd(II), and the ΔG, ΔH, and ΔS values calculated were -0.33 kJ/mol, 26.29 kJ/mol, and 87.95 J mol^{-1} K^{-1}, respectively. The mechanisms of adsorption of Pd(II), Pt(IV), and Au(III) were confirmed by XPS. © 2006 Wiley Periodicals, Inc. J Appl Polym Sci 101: 631–637, 2006

Key words: heteroatom-containing polymers; resins; adsorption

INTRODUCTION

Polymer-supported noble metal catalysts have many advantages such as high optical catalytic activity, ready separation from products after reaction, and maintaining optical catalytic activity without any remarkable loss after several times of reuse. Therefore, they have been widely applied in the hydrogenation reactions of alkylenes, dienes, alkynes, and nitroaromatics,[1–3] the selective oxidation of tetrahydrofuran (THF) into γ-butyrolactone,[4] and the asymmetric hydrogenation of *o*-cresol into (S)-2-methyl-cyclohexanone.[5] Experimental results showed that product and optical yields were greatly affected by many factors such as noble metal loading in the resins, structure of the chelating group, solvent quality, and reaction temperature. To investigate the effect of the structure of supports on reaction activity, we designed and synthesized a new chelating resin containing S and N heterocycles, polystyrene-supported 2,5-dimercapto-1,3,4-thiodizazole (PS-BMT).

According to Pearson's hard and soft acid–base concept, selective sorbents that are promising for sorption of noble metal ions are expected from polymers containing functional groups with donor N and S atoms. Chelating resins containing sulfur and nitrogen atoms possess excellent adsorption and selectivity properties for noble metal ions.[6–23] Therefore, many efforts have been made to prepare these types of resins. Because of their chelating nature with metal ions, these types of chelating resins are widely used in the preconcentration, separation, recovery, and hydrometallurgy of metals. There are two nitrogen atoms and three sulfur atoms in the structure of 2,5-dimercapto-1,3,4-thiodiazole ($C_2H_2N_2S_3$, BMT), which can chelate metal ions such as bismuth, copper, and lead. It would be expected that a chelating resin containing a functional group of BMT would have excellent adsorption properties toward metal ions. In the present study, we synthesized a type of chelating resin that contained BMT groups and investigated the adsorption properties for adsorbing Pd(II), Pt(IV), and Au(III).

EXPERIMENTAL

Reagents

Commercial macroporous chloromethylpolystyrene-*co*-divinylbenzene beads (PSC, with a degree of

Correspondence to: R. Qu (qurongjun@sohu.com or qurongjun@eyou.com).

Contract grant sponsor: Postdoctoral Science Foundation of China; contract grant number: 2003034330.
Contract grant sponsor: Science Foundation for Mid-Youth Elite of Shandong Province.
Contract grant sponsor: Nature Science Foundation of Shandong Province; contract grant number: Y2005F11.
Contract grant sponsor: Educational Project for Postgraduate of Yantai Normal University; contract grant number: YD05001.
Contract grant sponsor: Science Foundation of Yantai Normal University; contract grant number: 032912, 20052901, and 042920.

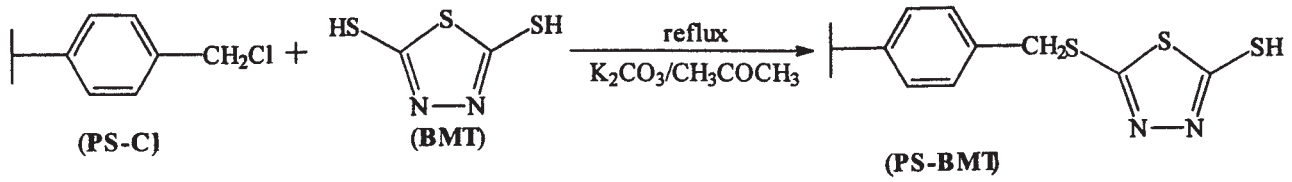

Scheme 1 Route of synthesis of PS-BMT.

crosslinking of 10% DVB and a chlorine content of 19.85%) were purchased from the Chemical Factory of Nankai University, Tianjin, China. Before use, the PSC was further purified by washing thoroughly to remove surface impurities using a procedure described in Dong et al.[19] BMT, $PdCl_2$, $HAuCl_4$, and H_2PtCl_6 were purchased from Aldrich Chemical Co., Missouri, MO. The other reagents and solvents were reagent grade and were used without further purification.

Measurements

Infrared spectra were recorded on a Nicolet MAGNA-IR 550 (series II) spectrophotometer (test conditions: potassium bromide pellets, scanning 32 times, resolution 4 cm^{-1}). Chlorine content was measured as described in Farrall and Frechet.[24] The other elementary analyses were carried out by the Central Laboratory of Elemental Research Institute of Nankai University. X-ray photoelectron spectroscopy (XPS) was recorded on a PHI1600 ESCA system made in the United States (test conditions: MgKα (1253.6 eV), power 200.0 W, resolution 187.85 eV). Quantitative and qualitative analyses were carried out by special data treatment software for this instrument. The concentration of metal ions was measured online on a GBC-932 atomic absorption spectrophotometer (AAS) made in Australia. The total energy and charge distribution of the model compound were calculated on a SGI O2™ workstation, using the charge equilibration method, Accelrys Cerius^2 version 4.2, MatSci software, OFFSETUP module, and DREIDING 2.21 force field.

Synthesis of polystyrene-supported BMT resin (PS-BMT)

The route of the synthesis of PS-BMT is described in Scheme 1. Added to a one-necked flask were 1.0 g of PS-Cl, 1.628 g of bismuththiol I (BMT), 4.0 g of K_2CO_3 powder, and 20 mL of acetone. With magnetic stirring, the mixture was refluxed for 8 h. The solvent acetone was distilled, and then 100 mL of distilled water was added to dissolve the salts. The polymeric product was filtered and washed with distilled water, a solution of 2% KOH, 1% hydrochloric acid, and finally with distilled water again. The product was transferred to a Soxhlet extraction apparatus for reflux–extraction in 95% ethanol for 10 h and then was dried under vacuum at 50°C over 48 h. Elemental analysis (%): Cl, 4.84; S, 19.51; N, 5.80. FTIR: $\nu_{C=N}$ 1381 cm^{-1}.

Adsorption kinetics

Batch tests were performed to determine adsorption kinetics. In a typical procedure 50-mL Pyrex glass tubes were prepared with the desired amounts of reagent solution (10 mL) and were placed in a thermostat-cum-shaking assembly. When the desired temperature was reached, a known amount of resin (0.05 g) was added to each tube, and the mixed solutions were mechanically shaken. At pre-deselected intervals, the solutions in the specified tubes were separated from the adsorbent, and the concentration of metal ions was determined by AAS. The amounts adsorbed were calculated according to eq. (1)

$$Q = \frac{(C_0 - C)V}{W} \tag{1}$$

where Q is the amount adsorbed (mmol/g); C_0 and C are the initial concentration and the concentration of the metal ions in solution at contact time t (mmol/mL), respectively; V is the volume (mL); and W is the weight of the chelating resin (g).

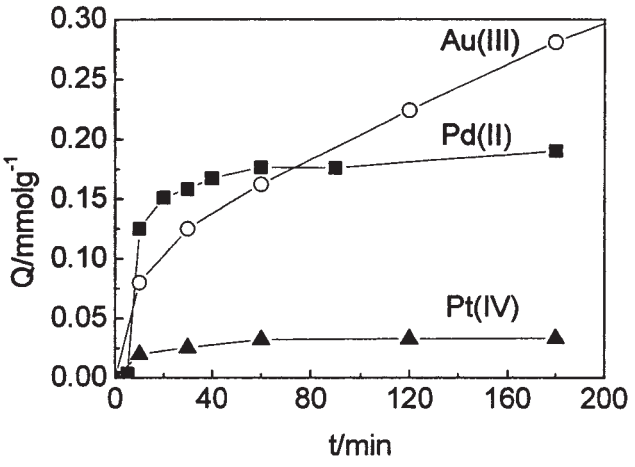

Figure 1 Adsorption rate curves of PS-BMT for Au(III), Pd(II), and Pt(IV) at 25°C (adsorption conditions: initial concentration, 220 ppm).

TABLE I
Adsorption Parameter of PS-BMT for Noble Metal Ions

Ion	Saturated adsorption capacity (mmol/g)	$t_{1/2}$[a] (min)	Distribution coefficient (mL/g)
Pd(II)	0.190	8.45	96.01
Pt(IV)	0.033	8.77	32.19

[a] $t_{1/2}$ is the time required to reach half the equilibrium adsorption amount.

Isothermal adsorption

Isothermal adsorption was also investigated by batch studies. A typical procedure was to use a series of 50-mL test tubes, each of which was filled with 10 mL of a metal ion solution of varying concentrations and adjusted to the desired pH and temperature. A known amount of resin (about 0.05 g) was added to each test tube and agitated intermittently for the desired time. Adsorption capacity also was calculated, using eq. (1), where C is the equilibrium concentration of a metal ion in solution.

RESULTS AND DISCUSSION

Rates and capacities of PS-BMT to adsorb Au(III), Pd(II), and Pt(IV)

The adsorption curves and parameters of adsorption by PS-BMT resin of Au(III), Pd(II), and Pt(IV) ions are shown in Figure 1 and Table I. The results show that the adsorption equilibriums for Pd(II) and Pt(IV) were established quickly, in 40–60 min, whereas the capacity to adsorb Au(III) continued to increase during the experiment, reaching 5.8 mmol/g after 36 days. This was probably because the Au(III) ions could be reduced continuously during adsorption, and its adsorption mechanism was different from those of Pd(II) and Pt(IV). Also, the saturated capacity and distribution coefficient of Pt(IV) were lower than those of Pd(II). A possible explanation for this is that Pd(II) and Pt(IV) were in the form of $PdCl_4^{2-}$ and $PtCl_6^{2-}$, respectively, and $PdCl_4^{2-}$ has a planar configuration, whereas $PtCl_6^{2-}$ has a octahedron configuration. Although the two kinds of chloro-coordinated anions both contained two negative charges, the planar-configured anion was more easily adsorbed by PS-BMT than the octahedron-configured anion.

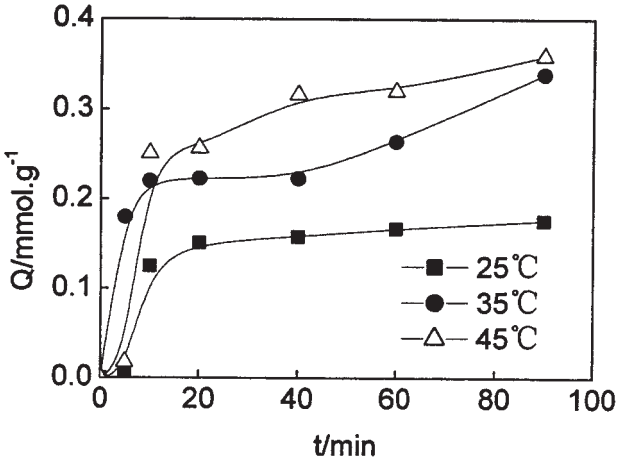

Figure 3 Adsorption kinetics of PS-BMT for Pd(II).

Effect of acidity on adsorption by PS-BMT of Au(III), Pd(II), and Pt(IV)

The adsorption capacities of Au(III), Pd(II), and Pt(IV) as a function of acidity were determined, and the results are presented in Figure 2. The adsorption ca-

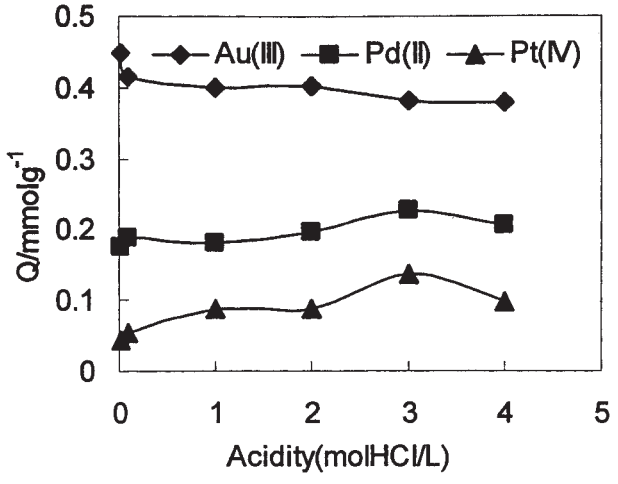

Figure 2 Effect of acidity on the adsorption of PS-BMT for Au(III), Pd(II), and Pt(IV) at 25°C (adsorption conditions: initial concentration, 220 ppm; contact time: 3 h).

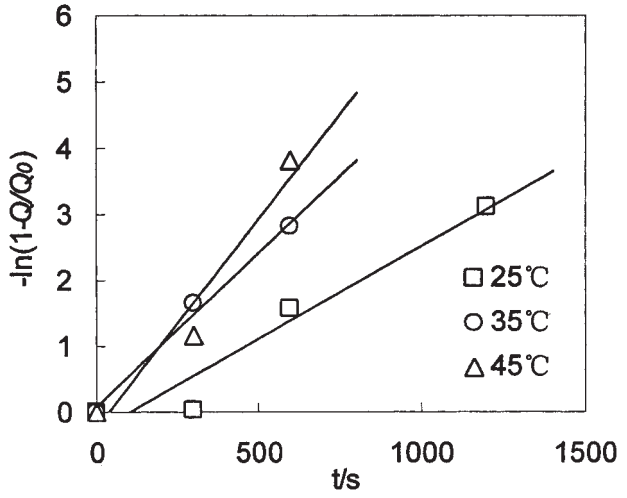

Figure 4 Relationship between $-\ln(1 - Q/Q_0)$ and adsorption time t.

TABLE II
Constants of Adsorption, k, and Correlation Coefficient R^2

Temperature (°C)	Constant rate of adsorption, k (s^{-1})	Correlate coefficient, R^2
25	2.8×10^{-3}	0.9404
35	4.7×10^{-3}	0.9898
45	6.4×10^{-3}	0.9509

pacity of Au(III) decreased slightly with increasing acidity, whereas that of Pd(II) and Pt(IV) increased slightly with increasing acidity, as can be seen in Figure 2. In general, adsorption was slightly dependent on acidity in the range of 0.01–4 mol HCl/L, indicating that PS-BMT resin could be used effectively in this acidity range.

Adsorption by PS-BMT of Pd(II)

Adsorption kinetics

Figure 3 shows the adsorption kinetics of Pd(II) at different temperatures. As shown in Figure 3, the adsorption capacity of Pd(II) increased with the prolonging of contact time. Because adsorption capacity did not significantly change after 40 min, in the following only data at this reaction time are discussed. Also, it can be seen that temperature had a significant effect on adsorption capacity, that is, adsorption capacity increased with increasing temperature. A possible explanation for this is that the resin was swollen more completely at higher temperatures, which made Pd(II) ions diffuse more easily into the inside of resin.

The results shown in Figure 4 were obtained by treating the results shown in Figure 3 with the Boyd equation, $-\ln(1 - Q/Q_0) = kt$, where Q is the amount adsorbed when contact time was t; Q_0 is the saturated adsorption capacity; k is the constant rate of adsorption; and t is the adsorption time. Both the linear relationship between $-\ln(1 - Q/Q_0)$ and t, shown in Figure 4, and R^2, shown in Table II, indicated that the process of PS-BMT adsorbing Pd(II) could be described by the Boyd equation, meaning that the adsorption obeyed the mechanism of liquid film diffusion control.[25]

According to the Arrhenius equation, $\ln k = -E_a/RT + A$, where k is the constant of adsorption. Plotting $\ln k$ against $1/T$, the results shown in Figure 5 were obtained. The apparent activation energy of adsorption, E_a, calculated from the linear slope was 32.67 kJ/mol. This low activation energy as compared to these of typical chemical reactions of 65–250 kJ/mol implied that the adsorption of PS-BMT for Pd(II) was a simple procedure.

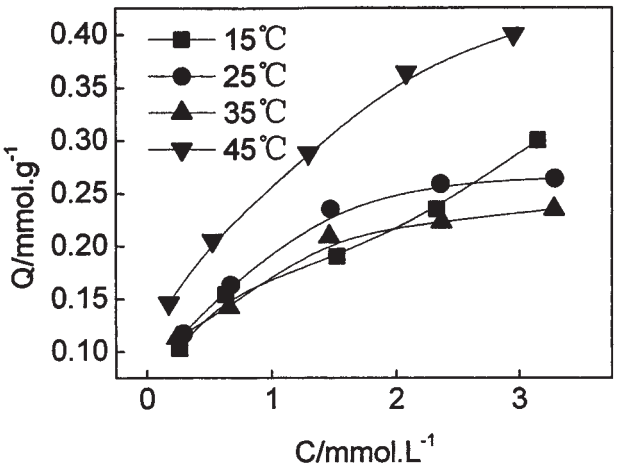

Figure 6 Adsorption isotherms of PS-BMT for Pd(II).

Isothermal adsorption

The adsorption isotherms of Pd(II) for three temperatures are presented in Figure 6. These data were ana-

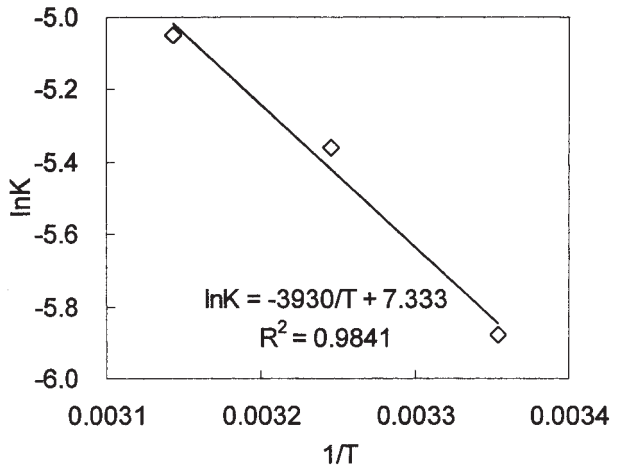

Figure 5 Relationship between $\ln k$ and $1/T$.

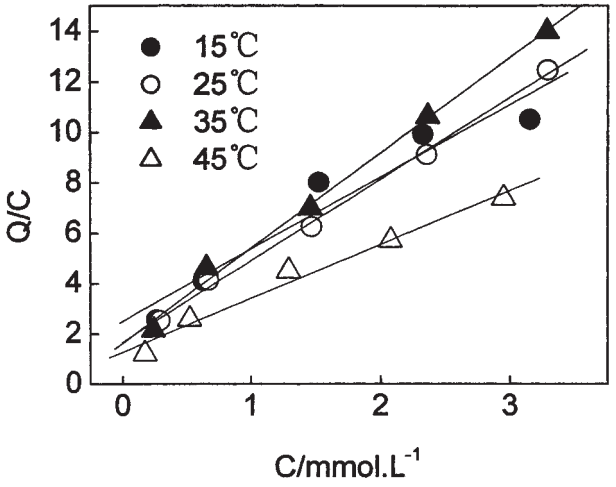

Figure 7 Langmuir isotherms of PS-BMT for Pd(II).

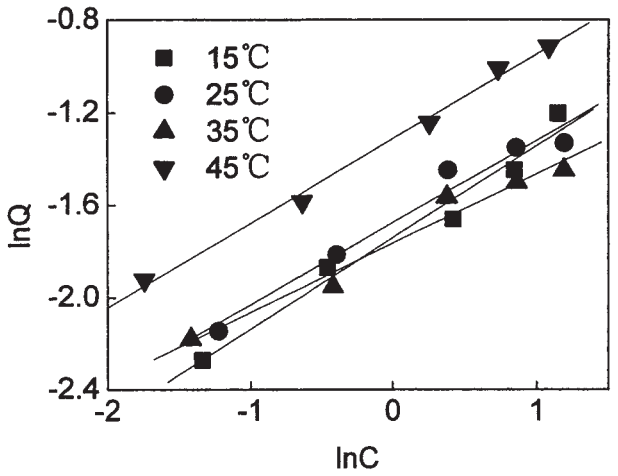

Figure 8 Freundlich isotherms of PS-BMT for Pd(II).

lyzed with the Langmuir [eq. (2)] and Freundlich [eq. (3)] equations, and the results are shown in Figures 7 and 8, respectively.

$$\frac{C}{Q} = \frac{1}{bQ_0} + \frac{C}{Q_0} \tag{2}$$

$$\ln Q = \ln K_F + \frac{1}{n}\ln C \tag{3}$$

where Q is the adsorption capacity (mmol/g); C is the equilibrium concentration of metal ions, mmol/mL; Q_0 is the saturated adsorption capacity (mmol/g); b is an empirical parameter; n is the Freundlich constant; K_F is the binding energy constant reflecting the affinity of the resin to metal ions. The Freundlich and Langmuir parameters are given in Table III. The correlation coefficients showed that, in general, the Langmuir model fitted the results slightly better than did the Freundlich model except at 15°C, indicating that all adsorption processes could be described by the Langmuir formula.

Changes in thermodynamic parameters, namely, free energy (ΔG), enthalpy (ΔH), and entropy (ΔS), also were calculated using eqs. (4)–(6), respectively, and are given in Table IV.

TABLE IV
Thermodynamic Parameters for Adsorption on PS-BMT Resin

Temperature (°C)	ΔG (kJ/mol)	ΔH (kJ/mol)	ΔS (J mol^{-1} K^{-1})
15	−0.33	26.29	87.95
25	−1.65		
35	−2.18		
45	−1.41		

$$\Delta G = -RT\ln K \tag{4}$$

$$\Delta H = -R\left(\frac{T_2T_1}{T_2 - T_1}\right)\ln\frac{K_2}{K_1} \tag{5}$$

$$\Delta S = \frac{\Delta H - \Delta G}{T} \tag{6}$$

where T, T_1, and T_2 are the Langmuir constants corresponding to temperatures of 15°C, 25°C, 35°C, and 45°C, respectively. A negative ΔG value confirmed the feasibility of the process and the spontaneous nature of the adsorption. The positive ΔH, which showed that the adsorption of Pd(II) by PS-BMT belonged to an endothermal process, was fitted to the results obtained from the adsorption kinetics.

PS-BMT mechanisms of adsorption of Au(III), Pd(II), and Pt(IV)

The results of XPS of PS-BMT before and after adsorption of Au(III), Pd(II), and Pt(IV) were investigated. The binding energy data of several elements are listed in Table V. The N_{1s} binding energy (400.08 and 401.1 eV) and the S_{2p} binding energy (162.61 and 164.71) showed that there were two combination states of nitrogen and sulfur respectively, in PS-BMT. In the two states of S, the binding energy of S_{2p} at about 162.61 eV increased by 0.31 and 0.33 eV after adsorption of Pt(IV) and Pd(II), respectively, and at 164.71 eV changed slightly (a decrease of only 0.07 and 0.11 eV, respectively), indicating that as an electron donor, only the former state of S was involved in coordinating with Pt(IV) and Pd(II). In the two states of N, the

TABLE III
Freundlich and Langmuir Constants for Pd(II) Adsorption on PS-BMT Resin at Different Temperatures

	Freundlich parameters			Langmuir parameters		
Temperature/°C	$K_F \times 10^3$	$1/n$	R_F^2	$Q_0 \times 10^3$	b	R_L^2
15	175.4	0.3970	0.9722	349.3	1.1468	0.9311
25	187.1	0.3555	0.9688	309.1	1.9482	0.9949
35	171.2	0.3006	0.9674	264.6	2.3397	0.9972
45	268.8	0.3656	0.9722	466.6	1.7014	0.9803

TABLE V
Binding Energy (eV) of Adsorption of PS-BMT for Au(III), Pd(II), and Pt(IV)

Samples	N_{1s} (%)	S_{2p} (%)	Au_{4f} (%)	Pt_{4f} (%)	Pd_{3d} (%)
PS-BMT	400.08 (84.46)[a]	162.61 (12.07)			
	401.73 (15.54)	164.71 (87.92)			
PS-BMT-Pt	400.12 (86.46)	162.92 (16.03)		73.16 (100)	
	401.64 (13.54)	164.64 (83.97)			
PS-BMT-Pd	400.14 (88.55)	162.94 (21.67)			337.59 (100)
	401.49 (11.45)	164.66 (78.33)			
PS-BMT-Au	397.87 (5.19)	164.59 (88.94)	85.24 (47.60)		
	400.20 (78.53)	168.91 (6.86)	87.00 (52.40)		
	401.83 (16.29)	171.08 (4.19)			
$PdCl_2$					337.8
H_2PtCl_6				75.6	
Au(0)[27]			83.86		
$HAuCl_4$[27]			87.33		

[a] Number in parentheses represents percent area of peak.

binding energy of N_{1s} changed slightly before and after adsorption of Pt(IV) and Pd(II), indicating that the two states of the N atom were not or were only lightly involved in coordinating with Pt(IV) and Pd(II). The binding energy of Pt_{4f} and Pd_{3d} decreased by 1.94 and 0.21 eV, respectively, after adsorption, showing that as electron acceptors, both kinds of metal ions were involved in coordinating with the S atoms of PS-BMT resin.

Unlike with the XPS of PS-BMT loading Pt(IV) and Pd(II), the binding energy peak of S_{2p} at 162.61 eV disappeared completely, and two new peaks, at 168.91 and 171.08 eV, appeared after adsorption of Au(III)—the peak area of the former (about 12.01%) was approximately equal to the sum of the latter two peaks (about 11.05%). It could be interpreted that this state of S was oxidized completely by Au(III) into —SO_2^- or —SO_3^-.[26] The binding energy of S_{2p} at 164.71 eV decreased only by 0.12 eV, indicating that this sate of S did not coordinate with Au(III), similar to that with Pt(IV) and Pd(II). The binding energy peak of N_{1s} at 400.8 and 401.73 eV increased by 0.12 and 0.10 eV, respectively, indicating that as electron donors of both states of the N atoms probably were involved in coordinating with Au(III) or were protonized by hydrogen ions. A new binding-energy peak of N_{1s} appeared at 397.87 eV, which probably was a result of tautomerization (see structure **II**) under adsorption conditions. The XPS showed there were two kinds of Au(III) states in the PS-BMT resin after adsorption. One kind of binding-energy peak appeared at 85.24 eV, which could be assigned as the characteristic peak of $Au_{4f7/2}$, which decreased by 2.09 eV in contrast with $HAuCl_4$, demonstrating that Au(III) participated in coordinating with the resin. The other peak, appearing at 87.00 eV, decreased only by 0.33 eV in contrast with $HAuCl_4$, indicating that this coordinating state of Au was different from the former one. From the XPS of PS-BMT loading Au(III), the characteristic binding energy peak of Au(0) formed by reduction of resin was not observed, although —S^- was oxidized into —SO_2^- or —SO_3^-. So it was justified to consider that Au(III) was reduced only to Au(I) by resin instead of to Au(0), and the binding energy peak of Au(I) in the complex with the resin probably was enshrouded by that of Au(III) in the complex with the resin.

From the XPS results it can be seen that only in the adsorption of Au(III) did the N atoms take part in the coordination. The N_{1s} binding energy did not increase greatly, which indicated that the coordination between the Au(III) ions and the N atoms was weak and that there probably was an ion-exchange action between them. Complexes such as —$N^+H[AuCl_4]^+$ may be formed during the adsorption of Au(III). Because of the hydrophobicity of PS-BMT, the rate of ion exchange was low, which resulted in a continued increasing capacity of Au(III) to be adsorbed with the prolonging of contact time. Similar phenomena were not found during the adsorption of Pd(II) and Pt(IV), suggesting that the adsorption mechanism of Pd(II) and Pt(IV) was different from that of Au(III).

Theoretically, the reaction between PS-Cl and BMT could form three possible structures of PS-BMT, as shown in Scheme 2. To confirm the preferential conformation, the total energy of the model compounds (see structures I, II, and III in grid line) was calculated by molecular modeling. The results of energy minimization, shown in Scheme 2, indicated that of the three structures, structure I had the least total energy of structure I, suggesting that the resin would be mainly in the form of structure I. Then the charge distributions on the S and N atoms in structure I were calculated. The results demonstrated that the S and N atoms each had two states, which was in agreement with the results of XPS. The negative charge was mainly in the S and N atoms, indicating these atoms had the donor capability to coordinate with metal ions.

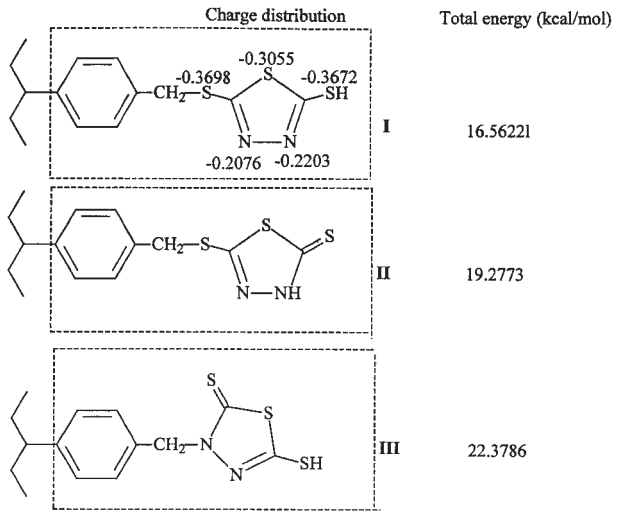

Scheme 2 Possible structures of PS-BMT resin, charge distribution, and total energy of model compound.

CONCLUSIONS

Polystyrene-supported 2,5-dimercapto-1,3,4-thiodiazole (PS-BMT) was synthesized from 2,5-dimercapto-1,3,4-thiodiazole and macroporous chloromethylpolystyrene via substitution reaction. The capacity of PS-BMT to adsorb Pd(II) and Pt(IV) was 0.190 and 0.033 mmol/g, respectively, and its adsorption capacity for Au(III) continued to increased with prolonged contact.

The adsorption dynamics of Pd(II) showed that adsorption was controlled by liquid film diffusion and that the apparent activation energy, E_a, was 32.67 kJ/mol. The Langmuir model described the isothermal process of Pd(II) better than did the Freundlich model; the ΔG, ΔH, and ΔS values calculated were -0.33 kJ/mol, 26.29 kJ/mol, and 87.95 J mol^{-1} K^{-1}, respectively.

The mechanisms of adsorption for Pd(II), Pt(IV), and Au(III) were confirmed by XPS. The adsorption mechanism for Au(III) was different from those of Pd(II) and Pt(IV). There were two combination states of nitrogen and sulfur in PS-BMT according to the results of XPS and the molecular modeling calculation. During the adsorption of Au(III), these ions coordinated with both S and N atoms, and some Au(III) ions were reduced to Au(0). Pd(II) and Pt(IV) ions only coordinated with S atoms, and no redox reactions occurred during adsorption.

References

1. Xavier, R.; Mahadevan, V. J Polym Sci Part A: Polym Chem 1992, 30, 2665.
2. Selvaraj, P. C.; Mahadevan, V. J Polym Sci Part A: Polym Chem 1997, 35, 105.
3. Sedláček, J.; Pacovská, M.; Rédrová, D.; Balcar, H.; Biffis, A.; Corain, B.; Vohlídal, J. Chem A Eur J 2002, 8, 366.
4. Wang, T.-J.; Ma, Z.-H.; Huang, M.-Y.; Jiang, Y.-Y. Polym Adv Tech 1996, 7, 88.
5. Mao, B.-W.; Zhao, A.-G..; Huang, M.-Y.; Jiang, Y.-Y. Polym Adv Tech 2000, 11, 254.
6. Chen, Y.-Y.; Lu, B.-X.; Chen, X.-W. J Macromol Sci Chem 1998, A25, 1443.
7. Chen, Y.-Y.; Cai, G.-P.; Wang, N.-D. J Macromol Sci Chem 1990, A27, 1321.
8. Chen, Y.-Y.; Yuan, X.-Z. Reac Polym 1994, 23, 165.
9. Chen, Y.-Y.; Hua, F.; Wu, X.-B. Polym Commun 1985, 5, 355.
10. Chen, Y.-Y.; Dai, Z. T. Acta Polym Sin 1989, 2, 146.
11. Bozena, N. K.; Dorota, J.; Andrzej, W. T.; Wieslaw, A. React Funct Polym 1999, 42, 213.
12. Bozena, N. K.; Dorota, J.; Andrzej, W. T.; Wieslaw, A.; Barbara, P. React Funct Polym 1998, 36, 185.
13. Dorota, J.; Wieslaw, A.; Andrzej, W. T.; Bozena, N. K. Solv Extra Ion Exc 1999, 17, 613.
14. Chang, X.-J.; Luo, X.-Y.; Xing, S.-Z.; Zhao, X.-B.; Lu, Y.-H. Chem J Chin Univ 1988, 9, 574.
15. Xu, Y.-W.; Zhang, C.-C.; Dong, S.-H. Chin J Appl Chem 1988, 5, 74.
16. Xu, Y.-W.; Zhang, C.-C.; Dong, S.-H. Acta Polym Sin 1989, 1, 109.
17. Dong, S.-H.; Tang, W.-X. Acta Polym Sin 1990, 1, 13.
18. Dong, S.-H.; Tang, W.-X.; Hu, Y.-H. Acta Polym Sin 1990, 2, 142.
19. Dong, S.-H.; Hu, Y.-H.; Zhao, Y.-M.; Zhang, W.-H.; Xu, Y.-W. J Wuhan Univ (Nat Sci Ed) 1995, 41, 161.
20. Hu, Y.-H.; Li, H.-P.; Dong, S.-H. J Wuhan Univ (Nat Sci Ed) 1995, 41, 401.
21. Dong, S.-H.; Wang, F.-H.; Li, J.-N.; Xu, Y.-W. J Wuhan Univ (Nat Sci Ed) 1990, 1, 119.
22. Qu, R.-J.; Liu, C.-P.; Ruan, W.-J.; Sun, L.; Liu, Q.-J. Chin J Mater Res 1999, 13, 51.
23. Rupal, S.; Surekha, D. Talanta 1998, 45, 1089.
24. Farrall, M. J. Frechet, J. M. J. J Org Chem 1976, 41, 3877.
25. Boyd, G. E.; Adamson, A. W.; Meyers, L. S. J Am Chem Soc 1947, 69, 2836.
26. Liu, S.-H.; Wang, D.-H.; Pan, C.-H. X-ray electron spectra analysis; Science Press: Beijing, 1988; p 175.
27. Liu, Y.-Y.; Fu, J.-K.; Hu, R.-Z.; Yao, B.-X.; Weng, S.-Z. Acta Microbio Sin 1999, 39, 260.